Article

Not peer-reviewed version

Rapid Estimation for the Maximum Remaining Capacity of Retired Lithium-Ion Batteries Based on CNN-CBAM-LSTM

Aqing Li , Penghao Cui , Yifei Cao * , Peng Zhou , Lei Yang , Guochen Bian , Zhendong Shao

Posted Date: 2 March 2026

doi: 10.20944/preprints202603.0063.v1

Keywords: retired lithium-ion batteries; maximum remaining capacity; rapid estimation; CNN-CBAM-LSTM

 doi:10.20944/preprints202603.0063.v1

Article

Rapid Estimation for the Maximum Remaining Capacity of Retired Lithium-Ion Batteries Based on CNN-CBAM-LSTM

Aqing Li [1], Penghao Cui [1], Yifei Cao [1,2,*], Peng Zhou [2], Lei Yang [3], Guochen Bian [4] and Zhendong Shao [5]

1 Key Laboratory of Advanced Perception and Intelligent Control of High-end Equipment, Ministry of Education, Anhui Polytechnic University, Wuhu 241000, China
2 School of Electrical Engineering, Anhui Polytechnic University, Wuhu 241000, China
3 School of Computer and Information, Anhui Polytechnic University, Wuhu 241000, China
4 Anhui Green Energy Technology Institute Co., Ltd., Hefei, 230061, China
5 Anhui Lvwo Energy Technology Co., Ltd., Lu'An, 230061, China
* Correspondence: yfcao@ahpu.edu.cn

Abstract

With the continuous increase in the number of retired lithium-ion batteries, accurately and quickly estimating their MRC has become a key challenge for the rapid sorting and secondary utilization of retired lithium-ion batteries. Conventional detection methods often suffer from low efficiency, prolonged detection cycles, and limited scalability for large-scale applications. To address these issues, this paper presents a fast MRC estimation method for retired lithium-ion batteries using a hybrid Convolutional Neural Network (CNN)-Conv Block Attention Module (CBAM)-Long Short-Term Memory (LSTM) architecture (CNN-CBAM-LSTM). The proposed approach integrates both factory-scale test data and laboratory experimental data to extract key voltage and capacity features from the initial 30-minute charging phase. Specifically, the CNN captures local temporal patterns, the LSTM models long-term dependencies in the time-series data, and the CBAM enhances feature representation by emphasizing critical characteristics. Experimental results demonstrate that the proposed method achieves MRC estimation within 30 minutes, significantly outperforming traditional approaches in terms of accuracy. The R^2 value increased to 99.42%, while the MAPE decreased to 1.55%. These results highlight the superior performance of the proposed method, which not only holds strong potential for rapid battery sorting and cascaded utilization but also exhibits broad applicability in large-scale battery health monitoring systems.

Keywords: retired lithium-ion batteries; maximum remaining capacity; rapid estimation; CNN-CBAM-LSTM

1. Introduction

The rapid global adoption of new energy vehicles has precipitated a sharp increase in retired lithium-ion batteries, making efficient and accurate assessment of their Maximum Remaining Capacity (MRC) a critical challenge for sustainable recycling and cascade utilization. China's retired power battery volume exceeded 40 GWh in 2023 and is projected to surpass 100 GWh by 2025 [1]. Batteries are typically retired when capacity degrades below 80% of the nominal value, yet they often retain sufficient MRC for secondary applications. Accurate MRC estimation is therefore essential to maximize resource efficiency. However, the current industrial standard,which need full charge-discharge cycle testing, requires up to 10 hours per battery, rendering it impractical for large-scale screening. Furthermore, prevalent MRC estimation methods predominantly rely on stable, long-term

 doi:10.20944/preprints202603.0063.v1

data from new batteries, which fails to address the complex and highly heterogeneous MRC distribution characteristic of retired battery populations.

Existing estimation techniques face significant limitations in this context. Model-based approaches, such as Electrochemical Impedance Spectroscopy (EIS), offer high accuracy but demand specialized instrumentation and strict laboratory conditions [2]. Incremental Capacity (IC) analysis is more accessible but remains highly sensitive to measurement noise and operational variability, limiting its robustness in real-world sorting scenarios [3,4]. While data-driven machine learning methods reduce dependency on physical models, they often require manually engineered features and extensive, full life-cycle training data [5]. Recent deep learning advancements, particularly Convolutional Neural Networks (CNNs), automate feature extraction from partial charging data [6,7], and their integration with Long Short-Term Memory (LSTM) networks improves temporal modeling [8]. Attention mechanisms, such as the Convolutional Block Attention Module (CBAM), further enhance model focus on discriminative segments of the input data [9]. Despite these progresses, a critical gap remains in developing a rapid, accurate, and generalizable solution tailored to the high variability and data-scarce nature of retired batteries on an industrial scale.

To bridge this gap, this paper proposes a novel, rapid MRC estimation framework that requires only the first 30 minutes of charging voltage–capacity data. Experimental validation demonstrates that the proposed method achieves an average relative error of 1.60% while constraining total detection time to 30 minutes, offering a significant advancement for high-throughput battery sorting and sustainable resource utilization.

2. Methodology

2.1. Data Acquisition

The existing public data set is mainly for the aging test of new batteries in the laboratory environment, such as the NASA PCoE datasets, the Oxford Battery Degradation Dataset, and various CALCE and EV-ageing datasets [10–13], which are widely used for battery modelling and prognostics These datasets provide valuable cycle-life, relaxation, and EIS measurements, but they rarely cover large, heterogeneous populations of retired power batteries with complex first-life usage histories. While those datasets lack the real diversified data of retired batteries, and the prediction accuracy decreases in the actual rapid detection of retired lithium batteries [14,15]. The samples used in this paper are all from the retired lithium batteries recovered in the factory. Through the joint experiment of the factory and the laboratory, the charge-discharge cycle data of 1648 retired batteries of the same type are collected, the cycle test step are shown in Figure 1. The MRC of batteries ranges from 70% to 100%. The basic information of lithium batteries was shown in Table 1.

Table 1. Battery Parameters.

Battery (Parameters)	Specifications (Value)	Battery (Parameters)	Specifications (Value)
Material	$LiFePO_4$	Dimensions	Φ32 mm × 80 mm
Rated Energy	24 Wh	Rated Capacity	7500mAh
Nominal Voltage	3.2V	Charge Cut-off Voltage	3.65V
Charge Cut-off Current	0.225A	Discharge Cut-off Voltage	2V

Figure 2 presents the integrated distribution of charge–discharge data for retired Lithium batteries across three maximum remaining capacity intervals: 70%–80%, 80%–90%, and 90%–100%. The data characteristics differ markedly among these ranges. In the high-MRC region (90%–100%), samples are the most abundant, with dense and well-defined voltage–capacity profiles that closely resemble those of fresh cells due to mild degradation; consequently, model predictions in this region tend to yield the smallest errors. The medium-MRC range (80%–90%) exhibits uniform data distribution and stable curve shapes, reflecting good capacity retention and consistency, thereby providing a reliable reference for modeling mid-capacity cells. In contrast, the low-MRC interval

 doi:10.20944/preprints202603.0063.v1

(70%–80%), which is a critical threshold for cascade utilization, shows originally sparse and scattered data owing to limited field-collected samples. To address this gap, laboratory multi-channel test data were introduced to supplement this interval, significantly increasing its sample density. This targeted augmentation results in a more balanced dataset across the full 70%–100% MRC span, offering robust support for the training and validation of the proposed MRC prediction model, particularly in the low-MRC regime.

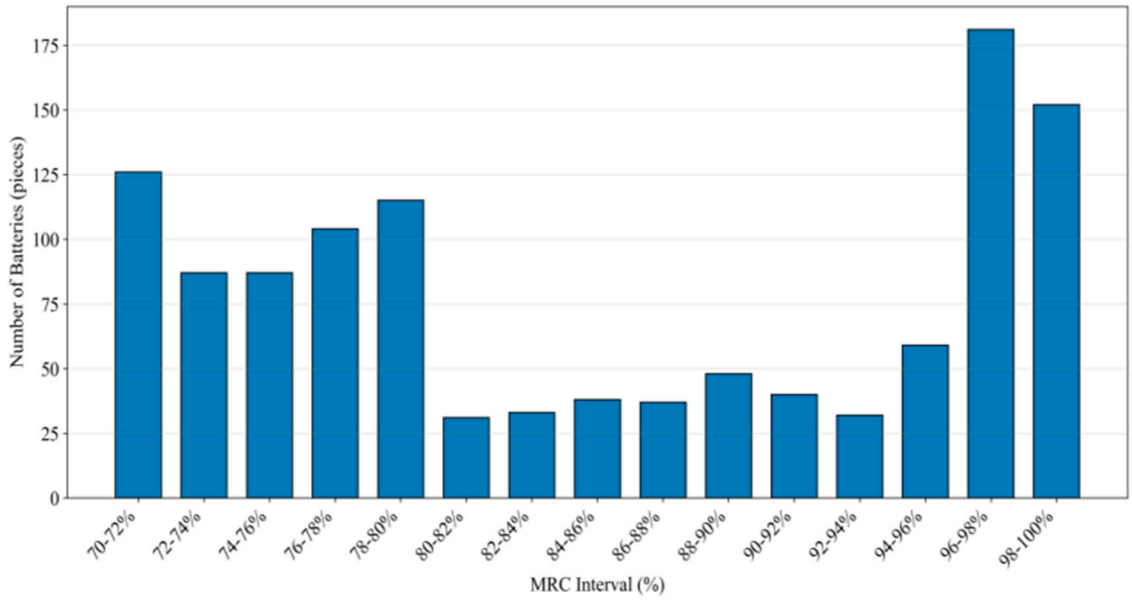

Figure 2. Charge-discharge data distribution of Lithium batteries with 70%-100% MRC.

2.2. Characteristic Analysis of Retired Lithium-Ion Battery

During the lifetime of a Lithium battery, the decrease in MRC serves as a direct measure of performance degradation. As the MRC declines, parameters describing battery performance and stability not only shift in magnitude but also show growing dispersion across cells with identical nominal MRC. In experimental tests, the constant-current (CC) charging/discharging duration, together with the applied current, directly indicates usable capacity. Upon ageing, the capacity-change rate in the voltage-plateau region varies significantly: heightened internal polarization, loss of active material lowering the plateau onset voltage, and shortened plateau duration collectively reduce the rate of capacity change. These dynamics are closely linked to the evolution of IC and dQ/dV curves, which are widely adopted as degradation indicators in IC -based analysis approaches.

Figure 3 presents dQ/dV curves for batteries across different MRC ranges. As MRC declines, both the capacity-change rate and the characteristic peaks within the voltage plateau exhibit marked evolution. Batteries with higher MRC display smooth, concentrated dQ/dV peaks, reflecting uniform electrochemical reactions and low polarization. At medium-low MRC levels, the curves become fluctuant with reduced reaction activity and increased polarization. Further degradation into the severe-aging range results in pronounced peak distortion and nonlinear jumps, indicating substantial active-material loss and elevated interfacial impedance. Consequently, the progression of dQ/dV peak position and magnitude provides a critical signature for characterizing and predicting battery MRC.

Figure 4a,b depict the charging process under full-voltage and partial-voltage conditions, respectively. The full-voltage charging cycle exhibits a clear dQ/dV-V peak with distinct characteristics along the complete curve. As the MRC declines, the effective charging current varies notably: low-MRC batteries demonstrate lower effective current and increased profile distortion, whereas high-MRC counterparts sustain higher and more stable current, reflecting superior charging performance and current-carrying capability.

 doi:10.20944/preprints202603.0063.v1

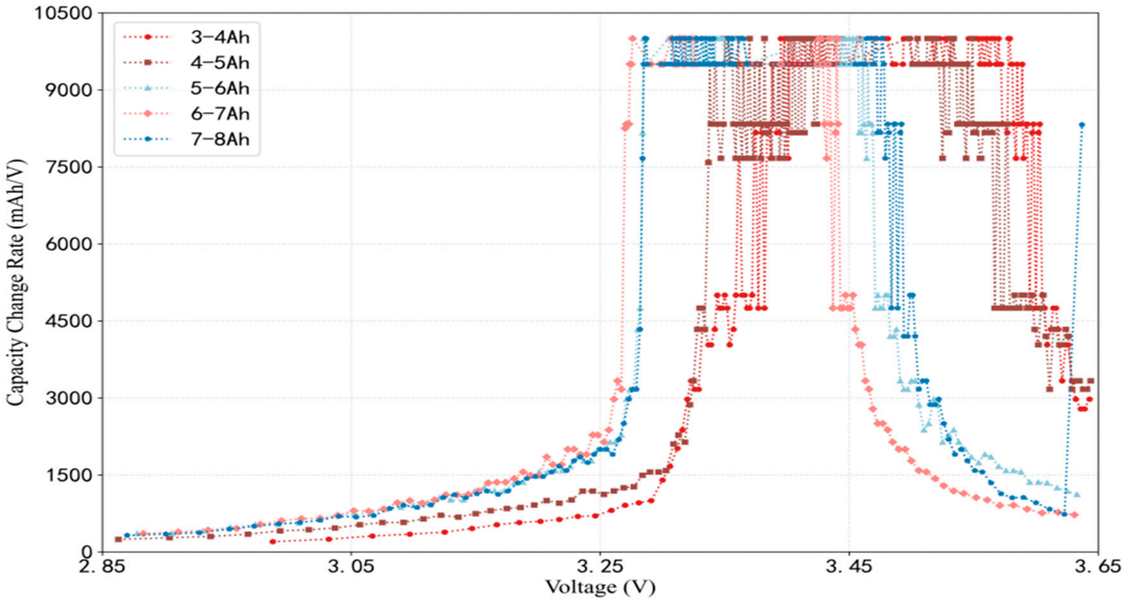

Figure 3. Comparison of incremental capacity change rates under different states of health.

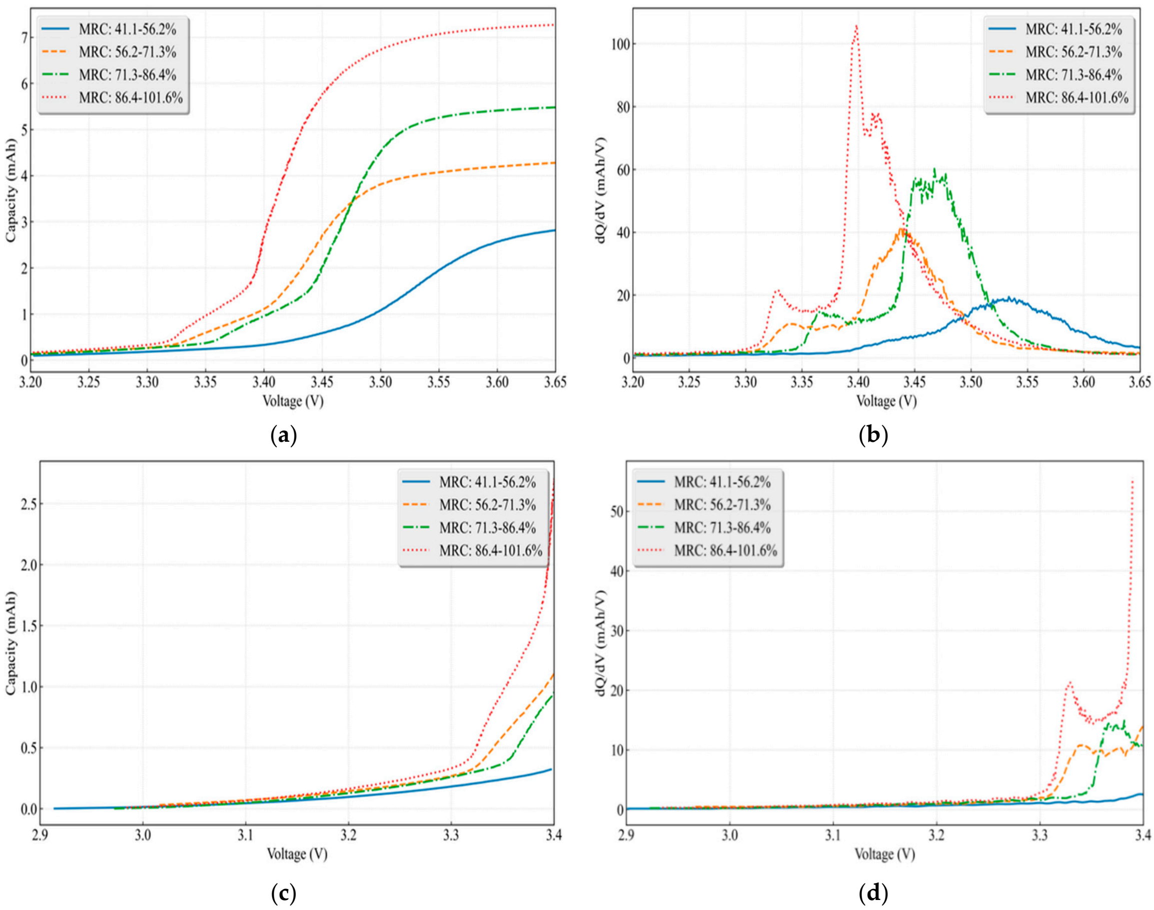

Figure 4. (**a**) Capacity-Voltage Curves of full CC-CV. (**b**) dQ/dV-V Curves of full CC-CV. (**c**) Capacity-Voltage Curves of partial CC-CV. (**d**) dQ/dV-V Curves of partial CC-CV.

Figure 4c,d show the variation of the capacity increment (dQ/dV) with voltage for high- and low-MRC batteries. For high-MRC batteries, the incremental-capacity curve is relatively smooth, indicating a stable charging process and good electrochemical uniformity. In contrast, for low-MRC batteries, the dQ/dV curve becomes steeper and more irregular, reflecting instability in the charging process and increased heterogeneity. Although the complete charging curve contains the full set of

 doi:10.20944/preprints202603.0063.v1

IC peaks, many peak characteristics are already visible within partial segments of the charging process. This observation suggests that it is feasible to use partial charging curves for model training and prediction, which can effectively extract key features for MRC assessment while avoiding the computational and data-processing burden associated with full-cycle curves.

3. Models and Methods

The input to the model consists of voltage and capacity data within the partial voltage window of 3.1 V-3.4 V. As depicted in Figure 5, these data are processed by two cascaded 1D convolutional layers for hierarchical feature abstraction.The first convolutional layer extracts local patterns from the voltage-capacity trajectories, with particular emphasis on dQ/dV characteristics that implicitly reflect changes in MRC and underlying electrochemical behavior. Since capacity increment evolves with aging, polarization, and state-of-charge (SOC) conditions, it is prioritized during feature learning [7]. Voltage features capture local variations such as rapid rises, quasi-constant plateaus, and minor fluctuations, whereas capacity-related features focus on the dynamic evolution of dQ/dV, especially shifts in peak shape and position across MRC levels. Features of dQ/dV are assigned higher weighting, enabling more accurate representation of aging- and polarization-induced capacity changes.

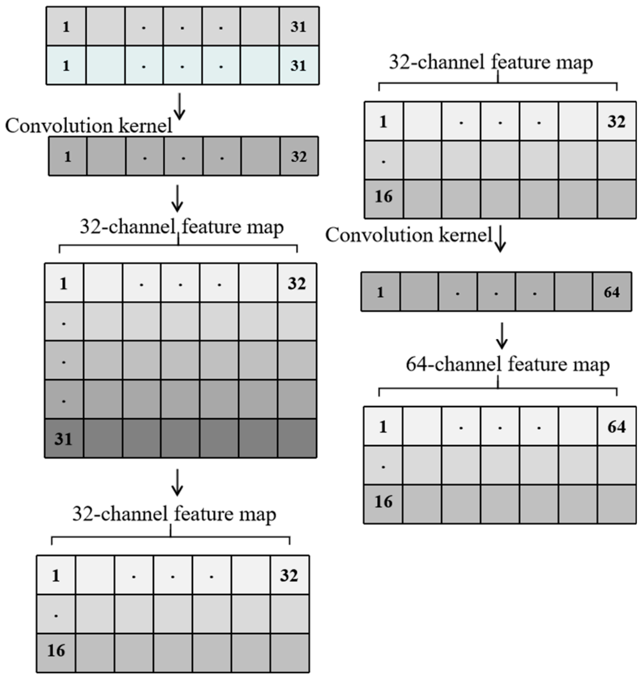

Figure 5. Convolutional feature extraction and transformation process of the CNN.

Following the feature extraction stage, a Convolutional Block Attention Module (CBAM) [9] is integrated to refine the learned representations. As illustrated in Figure 6, CBAM operates sequentially along the channel and spatial dimensions to enhance informative patterns and suppress redundant or less relevant features. Channel attention dynamically recalibrates feature maps by emphasizing channels most relevant to MRC estimation, while spatial attention aggregates contextual information and captures long-range dependencies across the sequential voltage–capacity data. This dual-attention mechanism enables the model to focus adaptively on critical regions and feature channels, which is particularly the dominant capacity-increment characteristics, thereby strengthening the representation of higher-order patterns related to aging modes, polarization effects, and transition-zone dynamics. The refined features offer improved discriminability and robustness for subsequent health assessment and capacity estimation.

Preprints.org (www.preprints.org) | NOT PEER-REVIEWED | Posted: 2 March 2026 doi:10.20944/preprints202603.0063.v1

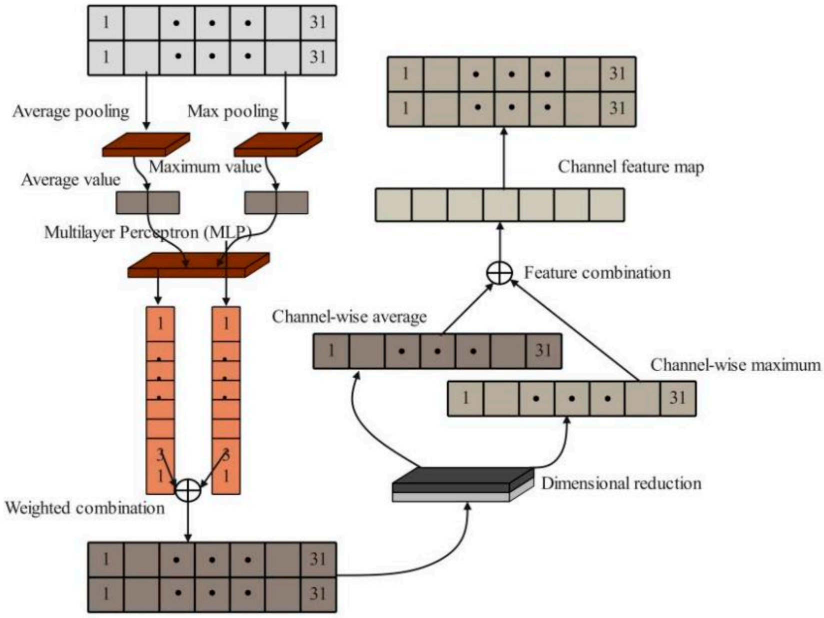

Figure 6. Structure and feature transformation process of the CBAM attention module.

The specific process is as follows:

Vertical Attention: Vertical Attention generates two height description vectors by performing global average pooling and global max pooling on the feature map along the width (W) direction.

$$F_{avg}^{V}=\mathrm{GlobalAvgPool}(F) \quad \text{and} \quad F_{max}^{V}=\mathrm{GlobalMaxPool}(F)$$

These two vectors represent the global information of the feature map along the width direction. They are then concatenated into a new vector.

$$F_V=[F_{avg}^{V},F_{max}^{V}]$$

The vertical attention weights are then generated through the convolutional layer followed by the Sigmoid activation function A_V:

$$A_V=\sigma(W_V F_V+b_V)$$

where W_V is the convolution kernel, b_V is the bias term, and σ is the Sigmoid activation function. The final vertical attention map A_V has values between [0, 1], representing the importance score of each spatial position along the width direction.

Horizontal Attention: Horizontal attention involves performing global pooling operations on the feature map along the height (H) direction to obtain two width description vectors. First, the input feature map F is transposed to F^T (exchanging the width and height of the feature map), and then global average pooling and global max pooling are applied to obtain two width description vectors.

$$F_{avg}^{H}=\mathrm{GlobalAvgPool}(F^T) \quad \text{and} \quad F_{max}^{H}=\mathrm{GlobalMaxPool}(F^T)$$

These two vectors are concatenated to form a new vector.

$$F_H=[F_{avg}^{H},F_{max}^{H}]$$

The horizontal attention weights are then generated through the convolutional layers followed by the activation function A_H:

$$A_H=\sigma(W_H F_H+b_H)$$

 doi:10.20944/preprints202603.0063.v1

where W_H is the convolution kernel, b_H is the bias term, and σ is the Sigmoid activation function. The values of the final horizontal attention map A_H are also in the range [0, 1], representing the importance scores of each spatial position along the height direction.

CBAM Attention Mechanism:CBAM generates the final attention map $A_{CBAM}$by integrating attention mechanisms in both the vertical and horizontal directions. This is achieved through element-wise multiplication, combining the two attention maps to emphasize important features:

$$A_{CBAM}=A_V \times A_H$$

Finally, the generated attention map $A_{CBAM}$is applied to the original feature map FFF to enhance key features and suppress irrelevant ones, thereby improving the accuracy and robustness of batteryMRC estimation.

Final Enhanced Feature Map: The feature map weighted by the CBAM attention mechanism is expressed as:

$$F_{enhanced}=A_{CBAM} \times F$$

Among them, $F_{enhanced}$ is the enhanced feature map, which highlights key features related to theMRC of the battery through the CBAM attention mechanism, suppresses irrelevant information, and thus improves the model's detection capability in battery health assessment.

The CBAM attention mechanism, through dual calibration, enhances the model's ability to focus on and represent crucial features, effectively reducing the impact of irrelevant background noise. It provides an efficient feature enhancement method by assigning feature weights across both channels and spatial dimensions in convolutional neural networks, emphasizing features with a high weight proportion to improve model accuracy.

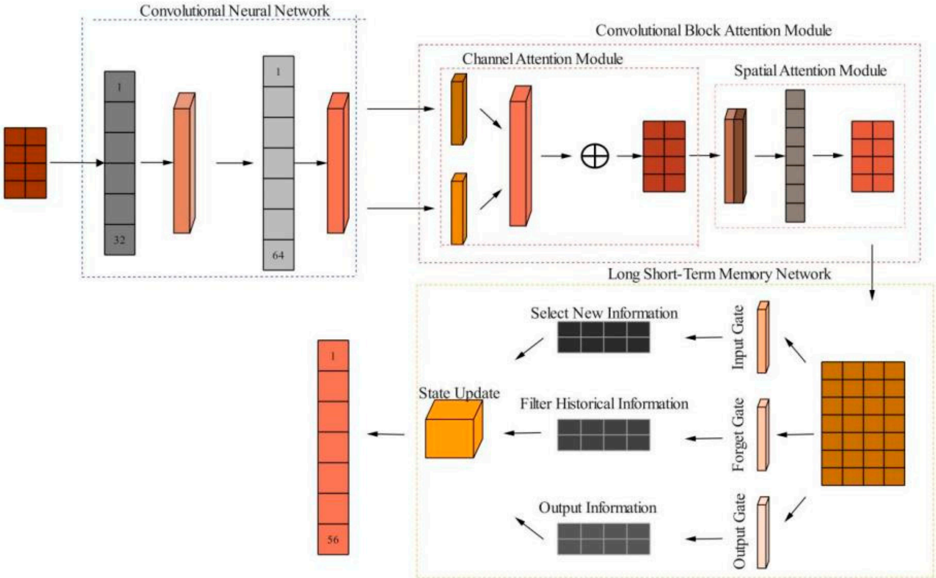

Figure 7. Overall structural framework of the CNN-LSTM-CBAM hybrid model.

The proposed deep learning framework employs a CNN-LSTM-CBAM architecture to reconstruct the complete charging capacity curve and estimate the MRC from partial voltage-capacity data. As shown in Figure 7, the model follows a structured three-stage pipeline: local feature extraction, temporal dependency modeling, and attention-based feature enhancement, collectively enabling accurate characterization of battery charging behavior.

The proposed hybrid network architecture takes 31 voltage–capacity (V–Q) pairs sampled from the initial charging segment as input, and outputs a sequence of 56 capacity points representing the reconstructed full charging profile. The model consists of four cascaded modules: a 1D convolutional feature extractor, a channel-spatial attention block, a temporal modeling unit, and a regression layer.

 doi:10.20944/preprints202603.0063.v1

First, a two-layer one-dimensional (1D) convolutional neural network (CNN) is employed to extract local nonlinear features, including slope variations and inflection points, from the input sequence. Each convolutional layer is followed by batch normalization and a ReLU activation function. The resulting features are then refined by a convolutional block attention module (CBAM), which sequentially applies channel attention (via global average- and max-pooling) and spatial attention (via a lightweight convolutional layer) to adaptively emphasize informative feature channels and salient temporal regions.

Subsequently, the attention-weighted features are passed through a two-layer long short-term memory (LSTM) network to capture long-range temporal dependencies in the V–Q evolution, thereby modeling the underlying electrochemical dynamics over the charging process. Finally, the LSTM outputs are projected through a fully connected layer to generate the 56-point capacity profile.

During training, the predicted curve is compared against the measured full charging profile to compute the loss. By jointly leveraging local spatial features and global temporal dynamics, the proposed architecture effectively aligns with recent advances in data-driven battery capacity estimation.

4. Results

To evaluate the proposed CNN-LSTM-CBAM model, we use a dataset combining laboratory measurements and industrial capacity-sorting line data. The input consists of 31 voltage-capacity feature points, and the output is a reconstructed full charging curve with 56 capacity points. Model performance is compared against two baselines (CNN-CBAM and CNN-LSTM) under identical dataset splits and training configurations. Evaluation metrics include the coefficient of determination (R^2), Mean Absolute Error (MAE), and Mean Absolute Percentage Error (MAPE).

To evaluate prediction accuracy, three models—CNN-CBAM, CNN-LSTM and the proposed CNN-LSTM-CBAM—are trained and tested under the same dataset split and training settings. Performance is assessed using several metrics, including the coefficient of determination (R^2), mean squared error (MSE), mean absolute error (MAE, in mAh) and mean absolute percentage error (MAPE).

As summarized in Table 2, the CNN-LSTM-CBAM model outperforms both baselines across all metrics. On the training set, it achieves an MAE of 96.48 mAh and MAPE of 1.55%, with an R^2 of 0.9942. On the test set, it maintains strong generalization, yielding an MAE of 98.78 mAh and MAPE of 1.60%. These results indicate the model's excellent capability in capturing the nonlinear characteristics of voltage-capacity curves while offering improved prediction accuracy and stability.

Table 2. Performance comparison of MRC prediction based on different models.

	Training set			Testing set		
Models	R^2 (%)	MAE (mAh)	MAPE (%)	R^2 (%)	MAE (mAh)	MAPE (%)
CNN	94.50	148.28	2.33	94.83	151.62	2.38
CBAM-CNN	92.94	184.50	2.96	96.51	128.03	2.07
LSTM-CNN	96.50	125.10	2.02	92.79	188.94	3.01
LSTM-CBAM-CNN	99.42	96.48	1.55	98.05	98.78	1.60

Figure 8 shows a point-by-point comparison of the prediction results and ground truth for the four models (CNN, CNN-CBAM, CNN-LSTM and CNN-LSTM-CBAM) on a typical test sample. It is evident that the prediction curve of the CNN-LSTM-CBAM model best matches the actual curve, with the smallest deviation among all models. In contrast, the other models exhibit larger local errors, especially near the voltage plateau regions, where capturing subtle capacity changes is more challenging.

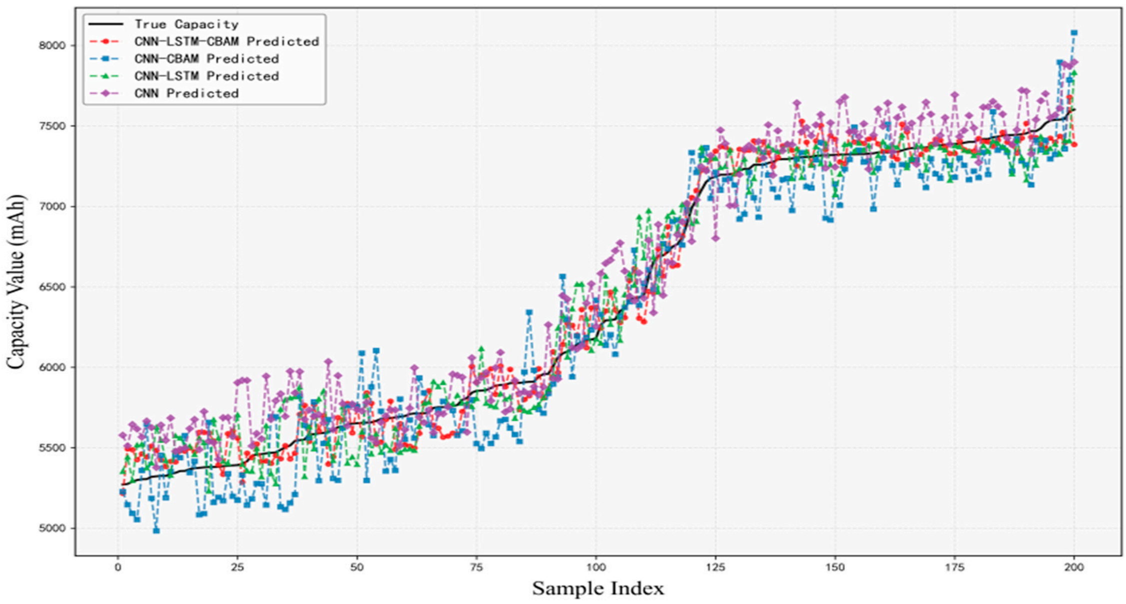

Figure 8. Comparison of Predicted Results and Actual Values for Different Models.

The CNN-LSTM-CBAM model exhibits the most accurate and stable performance, with an R^2 of approximately 0.9805 on this subset and average errors of MAE = 98.78 mAh and MAPE = 1.60%. These results confirm that, by combining the temporal modelling capability of LSTM with the feature-enhancement capability of CBAM, the proposed CNN-LSTM-CBAM model can effectively capture nonlinear degradation behaviour and sequence-dependent information in partial charging data. This leads to superior performance in MRC prediction compared with CNN-only and CNN-LSTM architectures, fully demonstrating the crucial role of the attention module in enhancing feature extraction and model accuracy.

Overall, the experimental results indicate that the proposed model not only achieves high fitting accuracy on the training data, but also maintains low prediction errors on unseen test data. This performance is competitive with or superior to other deep-learning-based approaches reported in the literature for capacity and SOH estimation, especially considering that only partial charging data are used for prediction.

5. Discussions

The proposed CNN-LSTM-CBAM framework provides a practical solution for rapid SOH estimation of retired lithium-ion batteries, balancing prediction accuracy with the computational efficiency required for industrial deployment. Unlike conventional grading methods that depend on full charge-discharge cycles or specialized electrochemical tests, our approach estimates the maximum remaining capacity (MRC) using only initial charging voltage-capacity data. This substantially reduces the per-cell testing time compared to multi-hour laboratory procedures. In deployment, the model performs online inference within seconds on standard test-platform hardware, meeting the throughput demands of large-scale battery screening.

The model achieves an average relative error below 2% across varied MRC levels and operating conditions. The hybrid architecture effectively combines the strengths of CNN and LSTM: the CNN extracts local nonlinear features, such as incremental-capacity peaks and voltage-plateau variations, while the LSTM captures the temporal dynamics of the charging process. The embedded Convolutional Block Attention Module (CBAM) further enhances robustness by adaptively highlighting critical feature intervals and suppressing irrelevant local fluctuations, leading to more stable predictions under diverse aging conditions.

Several limitations and future research directions are noted. First, model performance may degrade if directly applied to other battery chemistries due to differences in voltage profiles and aging

 doi:10.20944/preprints202603.0063.v1

mechanisms; transfer learning or chemistry-specific adaptation should be investigated. Second, data imbalance—particularly the scarcity of samples under severe aging (SOH < 60%)—affects prediction stability near end-of-life; expanding datasets through accelerated aging tests and field-operation data would improve robustness. Finally, incorporating additional features such as temperature and internal resistance could further enhance accuracy while maintaining real-time inference capability.

In summary, the proposed framework successfully bridges the gap between rapid screening and accurate prediction, providing a scalable and efficient tool for industrial reuse assessment of retired batteries. Future work will focus on extending chemistry coverage, enriching data diversity, and exploring multimodal feature fusion to broaden applicability.

6. Conclusions

This paper proposes a rapid Maximum Remaining Capacity (MRC) estimation framework for retired Lithium batteries, based on a hybrid CNN-LSTM-CBAM architecture. The method addresses the low efficiency and long testing cycles of conventional full charge-discharge or specialized laboratory techniques (e.g., EIS, ICA) by requiring only partial voltage-capacity data from the initial charging phase. The architecture synergistically combines convolutional layers for spatial feature extraction, LSTM units for temporal dynamic modeling, and a CBAM attention mechanism to focus on discriminative curve intervals.

Experimental results demonstrate that the model achieves an average relative error below 2% under a 3.5 A discharge rate while reducing the per-battery detection time from several hours to within 30 minutes. This significant improvement in throughput highlights the method's strong potential for industrial sorting applications.The proposed approach provides a scalable and deployable solution for rapid residual capacity assessment, supporting more intelligent cascade utilization and accurate valuation of second-life batteries. Future work will extend the framework to diverse battery chemistries, enhance datasets with extreme-aging samples, and incorporate multimodal physical indicators to further improve robustness and generalization.

Author Contributions: Aqing Li has made contributions in methodology, experiments, initial draft writing, and editing. Yifei Cao has made contributions in conceptualization, methodology, initial draft reviewing, and revising. Penghao Cui and Lei Yang have made contributions to software, data organization, writing review, and editing. Peng Zhou has made contributions to supervision, project management, funding acquisition, conceptualization, and methodology. Guochen Bian and ZhenDong Shao have contributed to investigations, data management, and resources. All authors have read and approved the final manuscript..

Funding: This work was supported by the Foundation of Science and Technology Research in Wuhu (2024kj018), and the Joint Opening Project of Anhui Engineering Research Center of Vehicle Display Integrated Systems and Joint Discipline Key Laboratory of Touch Display Materials and Devices in Anhui Province (VDIS&TDMD2024C02).

Data Availability Statement: The raw data supporting the conclusions of this article will be made available by the authors, without undue reservation.

Conflicts of Interest: The authors declare that they have no known competing financial interests or personal relationships that could have appeared to influence the work reported in this paper.

 doi:10.20944/preprints202603.0063.v1

References

1. Y. Zhang, Q. Tang, Y. Zhang, J. Wang, U. Stimming, A. A. Lee, Identifying degradation patterns of lithium ion batteries from impedance spectroscopy using machine learning, *Nature Communications*, vol. 11, 1706, 2020.
2. Y. Liu, L. Wang, D. Li, K. Wang, State-of-health estimation of lithium-ion batteries based on electrochemical impedance spectroscopy: A review, *Protection and Control of Modern Power Systems*, vol. 8, 39, 2023.
3. Afshari, Sajad Saraygord, Shihao Cui, *et al.*, On-board state of health monitoring of lithium-ion batteries using incremental capacity analysis with support vector regressionRemaining Useful Life Early Prediction of Batteries Based on the Differential Voltage and Differential Capacity Curves, *IEEE Transactions on Instrumentation and Measurement*, vol. 71, pp. 1-9, 2022.
4. M. Dubarry, D. Anseán, Best practices for incremental capacity analysis, *Frontiers in Energy Research*, vol. 10, 1023555, 2022.
5. K. A. Severson, P. M. Attia, N. Jin, N. Perkins, B. Jiang, Z. Yang, M. Chen, M. Aykol, P. K. Herring, D. Fraggedakis, *et al.*, Data-driven prediction of battery cycle life before capacity degradation, *Nature Energy*, vol. 4, pp. 383-391, 2019.
6. S. Shen, M. Sadoughi, M. Li, Z. Wang, C. Hu, Deep convolutional neural networks with ensemble learning and transfer learning for capacity estimation of lithium-ion batteries, *Applied Energy*, vol. 260, 114296, 2020.
7. Y. Li, K. Li, X. Liu, Y. Wang, L. Zhang, Lithium-ion battery capacity estimation—A pruned convolutional neural network approach assisted with transfer learning, *Applied Energy*, vol. 285, 116410, 2021.
8. Yifei Cao, Rui Wang, *et al.*, Rapid Prediction of Maximum Remaining Capacity in Lithium-Ion Batteries Based on Charging Segment Features and GA_DBO_BPNN, *batteries*, vol. 10, pp. 375-391, 2025.
9. S. Woo, J. Park, J.-Y. Lee, I. S. Kweon, CBAM: Convolutional Block Attention Module, in *Computer Vision - ECCV 2018*, Lecture Notes in Computer Science, vol. 11211, pp. 3-19, 2018.
10. Zhichao Li, Zhiguo Qu, *et al.*, Degradation mechanism of lithium-ion battery under appropriate in-plane temperature gradient, *Green Energy and Intelligent Transportation*, vol. 6, 100352, 2025.
11. M. Hassini, M. K. Tran, V. Panchal, *et al.*, Lithium-Ion Battery Data: From Production to Prediction, *Batteries*, vol. 9, 385, 2023.
12. B. Saha, K. Goebel, Battery Data Set, NASA Ames Prognostics Data Repository, Moffett Field, CA, 2007. (NASA PCoE Li-ion battery ageing dataset.)
13. C. A. Birkl, *Oxford Battery Degradation Dataset 1*, University of Oxford Research Archive (ORA), 2017. (Public Li-ion pouch-cell ageing dataset.)
14. CALCE, Battery Research Data, Center for Advanced Life Cycle Engineering, University of Maryland, public data portal, accessed 2025.
15. L. Cong, X. Zhang, Z. Chen, A review on health estimation techniques of end-of-first-use traction lithium-ion batteries, *Journal of Energy Storage*, 2024.
16. C. Wang, X. Tang, H. Wang, State estimation and aging mechanism of 2nd life lithium-ion batteries, *Electrochimica Acta* (or *Journal of Power Sources* - as per publisher record), 2023.
17. N. Wang, H. Li, Y. Zhang, Echelon Utilization of Retired Power Lithium-Ion Batteries, *Batteries*, vol. 8, 96, 2022.
18. J. Zhu, S. Zhang, X. Chen, *et al.*, End-of-life or second-life options for retired electric vehicle battery packs, *Cell Reports Physical Science*, vol. 2, 100678, 2021.
19. H. Song, C. Zheng, J. Wang, An overview about second-life battery utilization for energy storage systems, *Energies*, vol. 17, 6163, 2024.
20. W. Kong, X. Zhang, Y. Zhao, Residual capacity estimation and consistency sorting of retired lithium batteries in cascade utilization process: A review, *Green Manufacturing & Operation*, 2025.
21. S. T. Mowri, Y. Kavanagh, D. C. S. Kuhn, *et al.*, Dataset for assessing the impact of first-life lithium-ion battery degradation on second-life performance, *Data in Brief*, 2025.
22. K. A. Fricke, P. Gasper, Y. Preger, *et al.*, An Accelerated Life Testing Dataset for Lithium-Ion Batteries with Constant and Variable Loading Conditions, NASA Technical Report, 2023.
23. F. Stroebl, J. Sturm, R. Fuchs, *et al.*, A multi-stage lithium-ion battery aging dataset using sector-relevant drive cycles, *Scientific Data*, vol. 11, 2024.

 doi:10.20944/preprints202603.0063.v1

24. G. Pozzato, A. Allam, S. Onori, Lithium-ion battery aging dataset based on electric vehicle real-driving profiles, *Data in Brief*, vol. 41, 107995, 2022.
25. S. A. Hasib, S. Islam, R. K. Chakrabortty, *et al*., A comprehensive review of available battery datasets, RUL prediction approaches, and advanced battery management, *IEEE Access*, vol. 9, pp. 86166-86193, 2021.